Hindawi
Advances in Materials Science and Engineering
Volume 2021, Article ID 5957847, 17 pages
https://doi.org/10.1155/2021/5957847

Research Article

Damage Characteristics of Polymer Plates under the Impact of the Near-Field and Contact Underwater Explosion

Shucan Liu,[1,2] Xiaohua Zhao,[1,2] Hongyuan Fang,[1,2] Xueming Du,[1,2] and Binghan Xue[1,2]

[1]*School of Water Conservancy Engineering, Zhengzhou University, Zhengzhou 450001, China*
[2]*National Local Joint Engineering Laboratory of Major Infrastructure Testing and Rehabilitation Technology, Zhengzhou 450001, China*

Correspondence should be addressed to Xiaohua Zhao; zhaoxh2014@126.com and Hongyuan Fang; zhaoxh@zzu.edu.cn

Received 24 April 2021; Accepted 10 June 2021; Published 7 July 2021

Academic Editor: Zhengyang Song

In order to study the damage characteristics of polymer plates under the impact of the underwater explosion, the underwater contact and near-field explosion tests of polymer plates were conducted using different explosive quantities. In this paper, eight polymer plates with the size of 500 mm × 500 mm × 60 mm were made, and eight groups of explosion tests were carried out by using the rock emulsion explosive and nonconductive detonators. The damage modes and spatial distribution characteristics of the polymer plate generated by the underwater contact and near-field explosion impact with different explosive quantities are compared and analyzed. In addition, the characteristics of the shock wave propagation in the plates are investigated. It can be observed that the main damage mode of polymer plate is overall damage under the contact underwater explosion. For the near-field explosion, the main damage mode changes to overall failure, and the damage of contact explosion to polymer plate is greater than that of underwater near-field explosion. The polymer plate can reduce and delay the shock wave effectively, but the effect decreases with the increase of explosive quantity in the underwater contact explosion.

1. Introduction

Polymer material, also known as polyurethane, consists of polyol, isocyanate, and other raw materials. Due to the characteristics of lightweight, high expansion, strong permeability resistance, good durability, rapid curing, no pollution, etc., the polymer materials are widely used in foundation trenchless repair engineering and other infrastructures, such as trenchless repair of drainage pipeline leakage and settlement [1, 2], antiseepage reinforcement of dam [3], and improvement of foundation [4, 5]. Therefore, it is of great engineering significance and theoretical value to study the damage characteristics of polymer plates under underwater explosions.

Previous scholars have carried out lots of research related to the static mechanical properties of polymers. For example, Saleh et al. [6] found that polymer materials have the characteristics of low viscosity, high strength after curing, strong chemical stability, etc. Wang et al. [7] conducted experimental research on the impermeability of polymer materials and found that polymer materials have good impermeability, which can meet the antiseepage requirements of water conservancy projects. Chen et al. [8] conducted a tear resistance test on polymer materials under different temperature, humidity, and freezing conditions, and the results showed that the polymer material has good durability. Harikrishnan and Khakhar [9] observed that with the increase of the initial temperature of monomer, the gelation and foaming reaction of polymer become faster, and the polymer material has high expansibility. Shi et al. [10] carried out experimental research on the influence of temperature on the compressive strength of polymer material and found that when the polymer density is less than 0.4 g/cm^3, the influence of temperature on the compressive

strength of materials is small. Li et al. [11] found that the mechanical properties of low-density polyurethane were almost unaffected when the geometric size changed. Guo et al. [12] conducted field test research on the diffusion characteristics of expansive polymer materials in soil and found that the polymer developed flaky fracture diffusion in soil and finally formed a wedge-shaped section in the cracks. Wang et al. [13] studied the diffusion and reinforcement law of polymers in silt under different pressures and found that polymers can effectively reduce the porosity of soil to improve the properties of soil. Valentino et al. [14] studied the mechanical properties of two different types of polyurethane through experiments and found that the higher the restraint stress in the expansion stage of polyurethane, the higher the density after hardening. Saha et al. [15] conducted quasi-static compression tests on polyurethane foams with different densities and microstructures at different strain rates. By establishing stress-strain response under different strain rates, it is seen that the peak stress and energy absorption depend on the density of polyurethane foam, the microstructure of foam, and the strain rate. The aforementioned research mainly focuses on the static mechanical properties of polymers, while research studies on the dynamic properties of polymers, especially under the impact of the explosion, are still in their infancy.

In the study of explosion impact, the field explosion test is a direct and effective method. A large number of in situ explosion tests of concrete structures have been carried out. For example, Kumar et al. [16] studied the damage resistance of reinforced concrete slabs under blast loading, analyzed the damage characteristics of reinforced concrete slabs under different explosive quantities, and found that with the increase of explosive quantity, the bending and unidirectional splitting of slabs changed more significantly. Wang et al. [17, 18] studied the damage characteristics of square reinforced concrete slabs under near blast conditions by means of experiment and numerical simulation and obtained the failure modes and corresponding damage criteria of square reinforced concrete slabs. Wu et al. [19] conducted outdoor blast failure tests to study the effect of the aluminum foam protection layer on the blast resistance of reinforced concrete slabs. Li et al. [20] conducted contact explosion tests on ultrahigh performance concrete slabs, and the research shows that ultrahigh performance concrete slab has better antiexplosion performance than an ordinary concrete slab. Yu et al. [21] conducted a contact explosion test on BFRP reinforced concrete slab and found that the high strength and flexibility of BFRP make BRCS have better antiexplosion performance. Ohkubo et al. [22] found that fiberboard can prevent the concrete slab from breaking and improve the antiexplosion performance of the concrete slab through the contact explosion test of the concrete slab. Most of the reported studies have analyzed the antiexplosion performance and damage mode of concrete structures under the condition of air explosion, but few have studied the damage performance of structures under the condition of an underwater explosion. Zhao et al. [23] conducted experimental studies on the damage characteristics of concrete slabs under air and underwater contact conditions and obtained the influence of explosive quantity, steel bar, explosive shape, and fixed boundary on the damage of concrete slabs. Yan et al. [24] studied the dynamic response and failure mode of reinforced concrete piles under near-field noncontact underwater explosion conditions by combining experimental and numerical methods and proposed the safe distance of reinforced concrete piles according to the underwater explosion load under different working conditions. Yang et al. [25] compared the field explosion test results with the numerical model and studied the influence of different section shapes on the antiexplosion performance of reinforced concrete columns under underwater explosions. The above research mainly focuses on the antiexplosion performance of reinforced concrete materials, while less attention has been paid to the explosion characteristics of polymer materials, especially under the underwater explosion load.

In this paper, the damage characteristics of polymer plates under underwater contact and near-field explosion conditions are studied by field explosion tests. The contact and near-field explosion tests of polymer plates were carried out: four underwater contact explosion tests (specimens C1–C4) and four underwater near-field explosion tests (specimens N1–N4). By comparing the failure mode and the time history curve of shock wave pressure of polymer plate under the condition of different explosive quantity and distance from blasting center, the damage characteristics of polymer plate under the impact of underwater explosion are investigated.

2. Experimental Setup

2.1. Specimen Preparation. The polymer material is nonaqueous reaction type two-component polyurethane foam. A total of eight polymer plates with the same material and size were made, and the size of the specimens is 500 mm × 500 mm × 60 mm. In order to simulate the performance of polymer materials in practical engineering effectively, the density of all specimens is chosen to be 0.2 g/cm^3. The compressive strength and bending strength of the density polymer plates are 2.96 MPa and 2.52 MPa, respectively. And the polymer material of this density is widely used in engineering applications such as dyke seepage prevention.

In this experiment, the mold injection molding method is used to make the polymer plate (see Figure 1(a)). The grouting mold was made of steel plate with a thickness of 10 mm. Holes were drilled around the steel plate to fix the upper and lower steel plates with bolts, and a grouting hole with a diameter of 4.5 mm was drilled on the upper surface of the mold. Before grouting, lubricating oil should be evenly applied on the inner wall of the mold, and the upper and lower steel plates should be fixed with bolts. The polyols and isocyanate with the same mass were injected into the mold through the spray gun. After the two components contacted, the nonaqueous chemical reaction occurred and the volume expanded rapidly in a short period of time. After grouting for 3 h, when the polymer in the mold was fully reacted and cooled, the steel plate was removed to take out the polymer plate specimen, as shown in Figure 1(b).

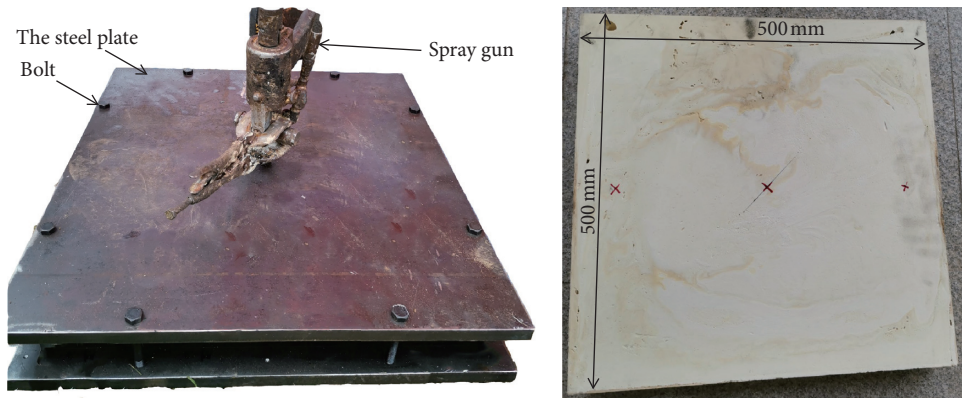

Figure 1: Specimen preparation. (a) Grouting mold. (b) Polymer plate specimens.

2.2. Explosion Load. Rock emulsion explosives with a density of 1.05 g/cm^3 and a brisance of 12 mm were used in the test. As shown in Figure 2(a), the explosive was weighed by an electronic balance with an accuracy of 0.01 g and a windshield. In order to avoid the loss of viscous emulsion explosive during weighing and use and ensure that the test charge is the designed charge, the explosive is wrapped in transparent plastic bags. It should be noted that the quality of the explosive in this explosion experiment is small (only 0–20 g), and the rock emulsion explosive has good fluidity, so the explosive has no regular shape. However, the irregular shape of the explosive has little effect on the experimental results and can be ignored (Zhao et al., 2018). As shown in Figure 2(b), nonconductive detonator was used in the test. The explosive in the detonator is Hexogen, and its power is equivalent to a 1 g rock emulsion explosive. The detonator was inserted into the explosive through a plastic bag to ignite the explosive.

2.3. Monitoring Equipment. In this test, the BLAST PRO impact tester was used to monitor and record the blast wave generated by the test (see Figure 3(a)). The instrument can provide 4 channels of fully parallel synchronous data acquisition and can work normally at −10°C~60°C. In this test, the manual operation mode was adopted in this test, with a collection rate of 4 M, a trigger balance of 0.5%, a sampling length of 0.1 s, a negative delay of 10 ms, and a collection range of 10 V for all four channels to ensure the integrity and accuracy of data as much as possible. As shown in Figure 3(b), the underwater shock wave sensor is TP series, the installation depth is 10 m, and the measuring range is 0–100 MPa, which meets the test requirements.

2.4. Experimental Setup. Because the density of the polymer plate is less than that of water, it needs to be fixed by fixing the device. Different sizes of channel steel were welded together to form a steel frame to fix the polymer plate and provided a fixed boundary for the polymer plate. Three bolt holes were, respectively, drilled on the top of the slot for fixing the polymer, and a gasket was placed between the polymer and the bolt. The binding force is provided by tightening the bolt and extruding the gasket to fix the polymer plate, as shown in Figure 4.

In order to ensure the explosion test of the polymer plate in the center of the water area, the steel pipes and supporting locks were used to build the frame meeting the test requirements, and the steel frame was erected and fixed on the frame by steel wire binding (see Figure 4). In the underwater contact explosion test, the explosive was fixed in the center of the polymer plate by wire. In the near-field explosion test, the horizontal distance between the explosive and the center of the polymer plate was 200 mm (see Figure 5). The center of the plate, the underwater shock wave sensors, and the rock emulsion explosive were in the same horizontal line. By using thin iron wires to bind the location of the sensitive components, the underwater shock wave sensors were, respectively, fixed at a distance of 800 mm and 1000 mm from the explosion source. And the sensitive element inside the underwater shock wave sensor was always on the same horizontal line as the center of the explosive. A rubber gasket was added at the binding place of the iron wire and steel pipe to ensure that the iron wire does not slide down. The four underwater shock wave sensors in the figure were numbered 1, 2, 3, and 4 from left to right, as shown in Figure 5. Under the condition of ideal water area, the time history curve of underwater explosion shock wave pressure was measured by using the shock wave sensor at the same level of the explosive.

2.5. Experimental Design. This test was designed to carry out eight underwater explosion tests, including four contact explosion tests (specimens C1–C4) and four near-field explosion tests (specimens N1–N4).

In order to study the damage characteristics of polymer plates under underwater near-field and contact explosion loads, underwater contact (C1–C4) and near-field (N1–N4) explosion tests were carried out on polymer plates with different mass rock emulsion explosives. In order to study the influence of the distance to the explosive center on the damage characteristics of the polymer plate under the underwater explosion load, the contact and near-field tests of

(a) (b)

Figure 2: Explosive devices. (a) Electronic balance. (b) Nonconductive detonator.

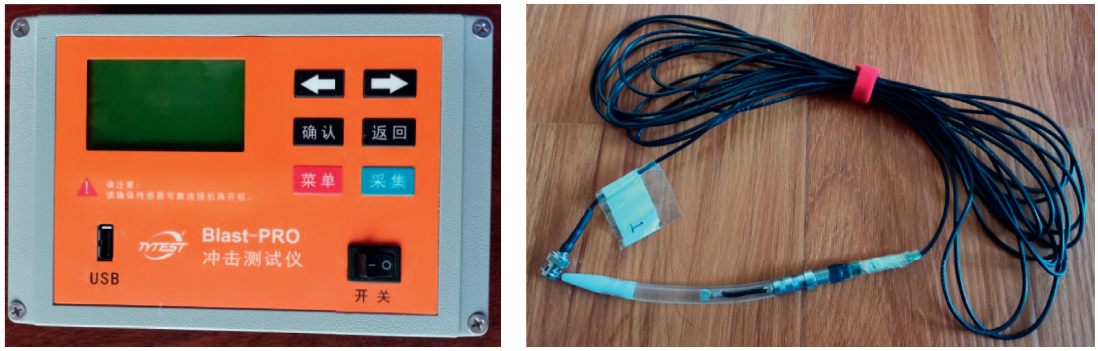

(a) (b)

Figure 3: Monitoring equipment. (a) Impact tester. (b) Underwater sensors.

the polymer plate were carried out with the same amount of rock emulsion explosive detonated by the detonator. The explosive power of the detonator is equivalent to 1 g rock emulsion explosive, so the influence of the detonator can not be ignored. For specimens C1 and N1, the contact and near-field explosion tests were carried out with a single non-conductive detonator, respectively. Explosion tests were carried out on eight polymer plate specimens under different working conditions, and the specific test details are shown in Table 1.

3. Underwater Contact Explosion Tests

In order to study the influence of explosive quantity on the damage characteristics of polymer plates under the action of underwater contact explosion load, underwater contact explosion tests were carried out on four polymer plates (C1–C4). In the test of specimens C1–C4, 0 g, 5 g, 8 g, and 20 g rock emulsion explosives were fixed at the center of the polymer plate and detonated by a single detonator, respectively (see Figure 6).

3.1. Failure Characteristics. When the explosive quantity is 0 g, i.e., the explosive load is only a single detonator, the local failure of the polymer plate C1 occurs. As shown in Figure 7, failure occurred in the middle of plate C1, the maximum length and width of the plate surface falling off area were 425 mm and 259 mm, respectively, and the specimen was broken into three independent parts. Under the action of contact explosion, the shock wave produced by the explosion directly acts on the polymer plate, and the compressive stress is higher than the compressive strength of the polymer material, so the polymer plate has a penetration failure and the surface has a spalling failure. Under the impact of a single detonator blast load, the residual area of the polymer plate

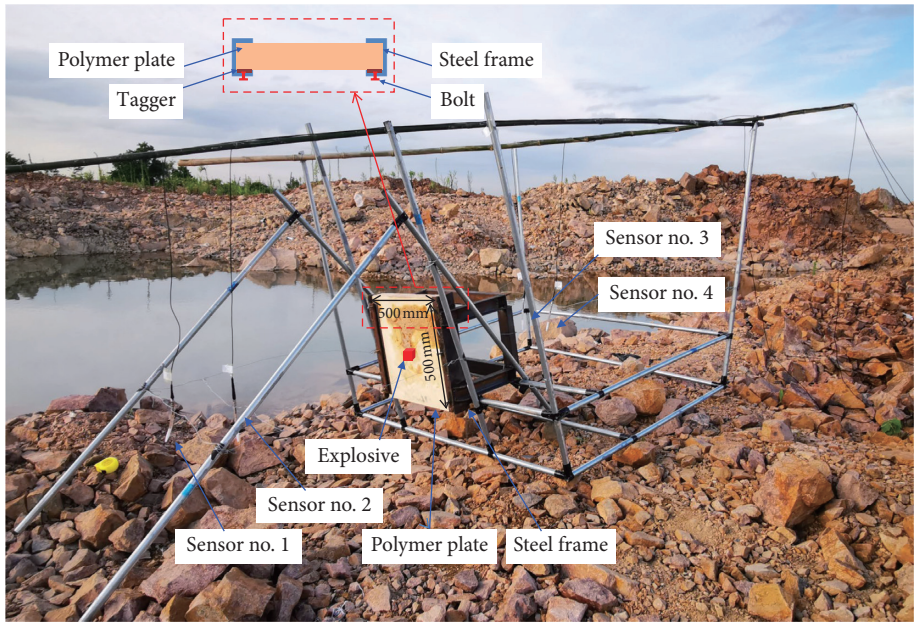

Figure 4: Arrangement of contact explosive test apparatus.

Table 1: Parameters of the underwater explosion tests.

Working condition	Dimension (mm)	Plate no.	Rock emulsion explosive (g)	Distance from blasting center (mm)	Detonation mode	Boundary condition
Underwater contact tests	500 × 500 × 60	C1	0	0	Single nonconductive detonator	Fixed
		C2	5	0	Single nonconductive detonator	Fixed
		C3	8	0	Single nonconductive detonator	Fixed
		C4	20	0	Single nonconductive detonator	Fixed
Underwater near-field tests	500 × 500 × 60	N1	0	20	Single nonconductive detonator	Fixed
		N2	5	20	Single nonconductive detonator	Fixed
		N3	10	20	Single nonconductive detonator	Fixed
		N4	20	20	Single nonconductive detonator	Fixed

accounts for 90.58% of the polymer plate area, the largest fragment area accounts for 76.56%, and the smallest fragment area accounts for 5.99% of the polymer plate area.

When a 5 g rock emulsion explosive is detonated, the impact energy generated by the explosion causes serious damage to the polymer plate. Due to the overpressure of shock wave generated by the explosion, there is a penetrating area with the size of 440 mm long and 500 mm wide in the middle of plate C2, and only five pieces of polymer fragments are left at the fixed boundary on the left and right sides (see Figure 8). The total area of the specimen residual fragments accounted for 30.07% of the polymer plate area, of which the maximum area and minimum area fragments accounted for 6.85% and 4.36%, respectively.

When the amount of explosive continues to increase to 8 g, plate C3 is completely broken into six independent fragments, and the remaining fragments are distributed around the plate (see Figure 9). The left and right fixed boundaries of plate C3 are broken and no longer complete. The experimental results show that the residual area of the plate accounts for 40.39% of the total area of the polymer plate; the largest fragment of the plate is located at the fixed boundary on the right side of the plate, accounting for 9.41%; the smallest fragment of the plate is located at the lower side of the plate, accounting for 3.28%.

When the explosive quantity continued to increase to 20 g, the polymer plate C4 was completely broken, and the smaller fragments floated on the water surface. When the

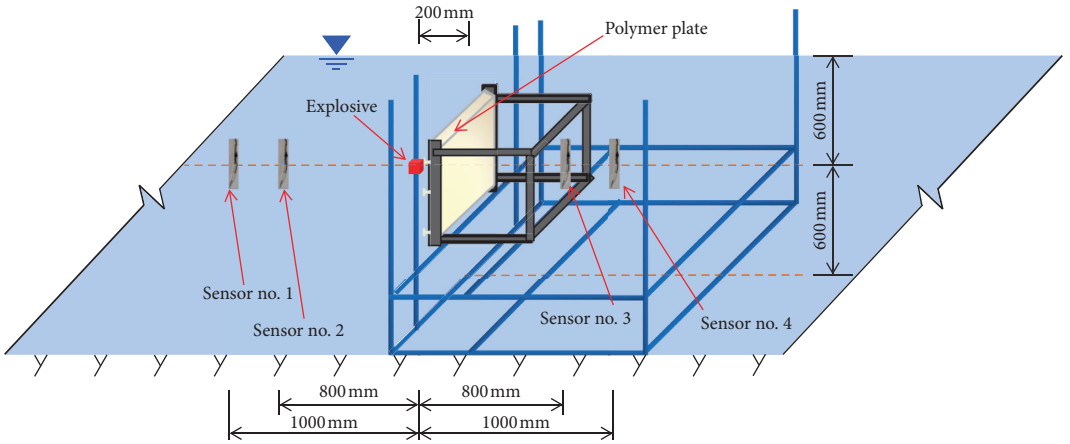

Figure 5: Schematic diagram of the near-field explosion test device.

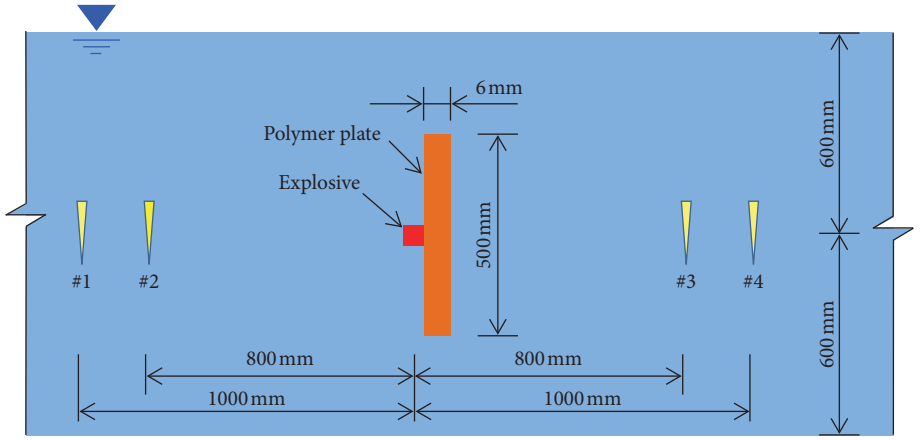

Figure 6: Schematic diagram of underwater contact explosion test.

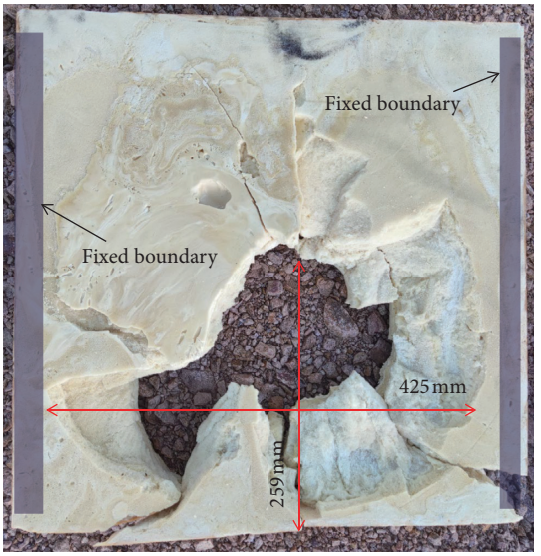

Figure 7: Test results of the polymer plate C1 under 0 g explosive (only one nonconductive detonator).

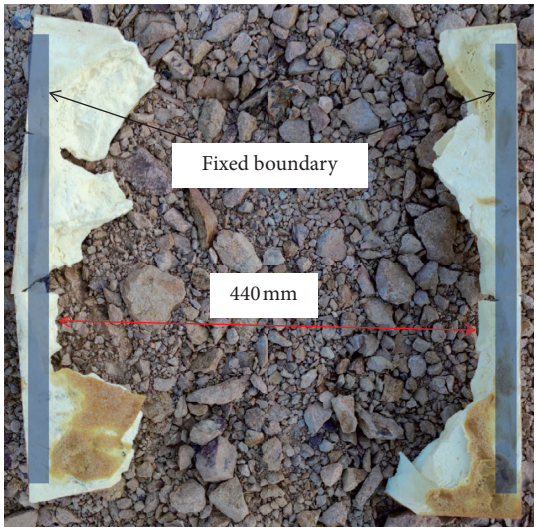

Figure 8: Test results of the polymer plate C2 under 5 g explosive.

Figure 9: Test results of the polymer plate C3 under 8 g explosive.

safety alarm was lifted, the fragments on the water surface had floated far away and could not be recorded.

It can be seen from Figures 7–9 that under the condition of underwater contact explosion, with the increase of explosive quantity, the damage mode of the polymer plate changes from local through damage to overall breakage, and the specimen is broken into pieces of different sizes, and the size of the pieces becomes smaller and smaller. The reason is that under the action of an underwater contact explosion, the shock wave generated by the explosion directly acts on the polymer plate, resulting in the penetration failure of the contact part.

When the explosive quantity is 0 g, 5 g, and 8 g, the residual area, maximum fragment area, and minimum fragment area of plate C1–C3 are counted, respectively, as shown in Table 2. The comparative analysis shows that the minimum fragment area of polymer plate decreases with the increase of explosive amount, and the minimum fragment area of C2 and C3 decreases by 27.18% and 45.33%, respectively, compared with C1.

3.2. Shock Wave Propagation Characteristics. In order to analyze the propagation of explosion shock wave propagation in the polymer plate under underwater contact explosion, four measuring points of 1–4 are set before and after the center of the specimen, as shown in Figure 10. In order to study the effect of polymer plate on shock wave reduction, two measuring points were arranged before and after the plate, and the propagation characteristics of shock wave before and after the polymer plate were compared and analyzed.

Figure 10 shows the time history curve of shock wave pressure before and after the center of polymer plate under the action of underwater single detonator contact explosion load and gives the specific position of the measuring point relative to the polymer plate and the peak value of the measuring point. It can be seen from the figure that the peak pressure of measuring point 2 on the same side of the emulsion explosive is the largest. In the initial stage of the shock wave, the pressure immediately reaches the peak value of 6.213 MPa. After the descending stage, the pressure increases again, reaches the second peak pressure, and then decays gradually and tends to be stable, and the second peak pressure is the bubble pulse load generated by bubble pulse. The distance between the explosion source and measuring points 2 and 3 is 800 mm, but the peak value of shock wave pressure of point 3 is 0.413 MPa, which is 93.35% lower than that of point 2. Measuring points 1 and 4 are 1000 mm away from the blasting center, and their pressure peaks are 3.408 MPa and 0.193 MPa, respectively. Compared with measuring point 1, the peak values at measuring point 4 attenuate by 94.34%, because most of the energy of the water shock wave propagating to the back of the plate is consumed by the damage of the specimen. The density of the polymer plate is lower than that of the water body, and the propagation velocity of the explosion shock wave in the polymer plate is lower than that in the free water body. Therefore, the peak time of measuring points 2 and 1 on the same side of the explosion source is earlier than that of measuring points 3 and 4 on the other side of the polymer plate, respectively. The time interval between measuring points 2 and 3 for the arrival of the peak pressure is 0.166 ms, and that between measuring points 1 and 4 is 0.225 ms, so the polymer plate can delay the propagation of the explosion shock wave.

When the explosive quantity is 5 g, the shock wave pressure curve at four measuring points is shown in Figure 11, which is similar to the shock wave pressure curve when the explosive quantity is 0 g. The pressure peak values of measuring points from large to small are 2, 1, 3, and 4, respectively. The peak value of point 3 decreases by 91.66% compared with point 2, and the peak value of point 4 decreases by 91.43% compared with point 1. The order of the peak pressure of measuring points 1–4 is the same as that of explosive quantity 0 g. The time interval between the peak

Table 2: Residual area of the polymer plate under contact explosion.

The explosive quantity	0 g	5 g	8 g
Residual area (mm^2)	226459	75186	100987
Maximum fragmentation area (mm^2)	191390	17131	23520
Minimum fragmentation area (mm^2)	14980	10908	8189
Residual area ratio (%)	90.58	30.07	40.39

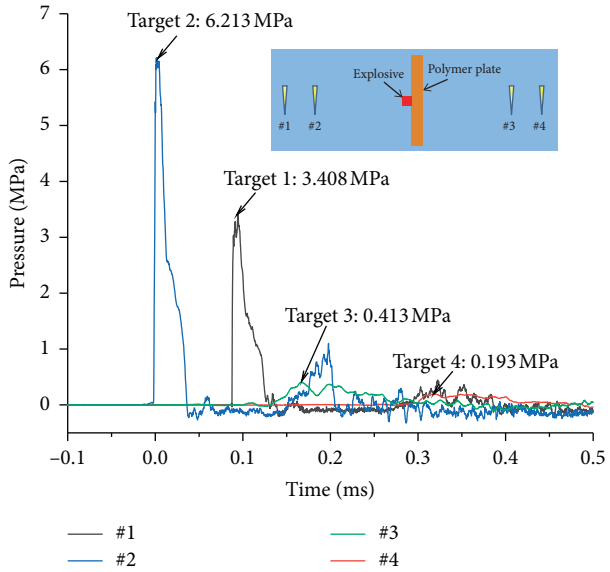

Figure 10: Shock wave pressure curve of the polymer plate C1 under 0 g explosive.

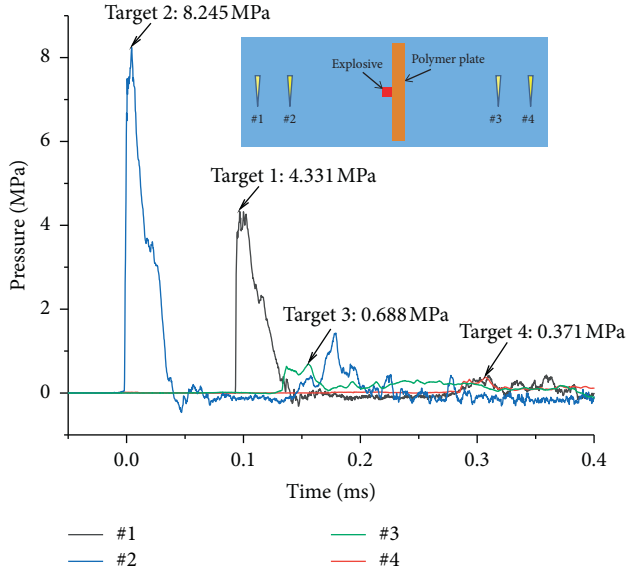

Figure 11: Shock wave pressure curve of the polymer plate C2 under 5 g explosive.

pressure of measuring points 2 and 3 is 0.151 ms, and that of measuring points 1 and 4 is 0.210 ms.

When the explosive quantity is increased to 8 g, the pressure time history curves of the four measuring points before and after the polymer plate C3 are shown in Figure 12. The peak pressure of measuring point 2 is the largest, which is 11.122 MPa. When there is a polymer plate between the measuring point and the explosion source, the peak pressure of the measuring point decays rapidly. The peak pressure of measuring point 3 decreases to 2.629 MPa, which decays 76.36% relative to measuring point 2; the peak pressure of measuring point 4 decays 75.42% relative to measuring point 1. The time sequence of measuring points 1–4 to reach the peak value is measuring points 2, 3, 1, and 4. The measuring points 2 and 3 closest to the explosion source reach the peak value first, followed by measuring points 1 and 4. The time interval between the peak pressure of measuring points 2 and 3 is 0.048 ms, and that of measuring points 1 and 4 is 0.095 ms.

Figure 13 shows the pressure time history curves of the front and back measuring points of the polymer plate under the action of 20 g explosive. Under a load of the underwater explosion, the pressure at the measuring point reaches the peak value instantaneously and then decays exponentially, and the decaying speed decreases gradually. Points 2 and 3 are closer to the explosion source, and the time to reach the peak pressure is earlier than measuring points 1 and 4. The time intervals between the peak pressure of measuring points 2 and 3 and that of measuring points 1 and 4 are 0.023 ms and 0.060 ms, respectively. It can be seen from Figure 13 that the peak values of measurement points 3 and 4 decrease by 66.29% and 73.82%, respectively, for measurement points 2 and 1.

It can be seen from Figures 10–13 that, under the same explosive quantity, the peak values of shock wave pressure at measuring points from large to small are measuring points 2, 1, 3, and 4, respectively. At the same distance from the explosion center, the peak pressure at measuring points 3 and 4 is much smaller than that at measuring points 2 and 1. As shown in Figure 14, under the action of underwater contact explosion, the polymer plate can reduce the explosion shock wave, and the effect is significant when the explosive quantity is small, but with the increase of explosive quantity, the reduction effect decreases rapidly. It can be seen from Figure 15 that, with the increase of explosive quantity, the energy of shock wave generated by explosion increases, resulting in the peak pressure at the measuring points gradually increasing, but the difference between the pressure peak values at the measuring points with the same distance from explosive center gradually decreases.

It can be seen from Figure 16 that when the amount of primary explosive increases from 0 g to 20 g, the time interval between the peak pressure of measuring point 2 and that of measuring point 3 decreases gradually, and the time interval decreases by 9.0%, 71.1%, and 86.1%, respectively, compared with that when the amount of primary explosive is 0 g. The time interval between the peak pressure of measuring point 1 and that of measuring point 4 gradually decreases with the increase of explosive quantity, and the time interval decreases by 6.7%, 57.8%, and 73.3%, respectively. With the increase of explosive quantity, the delay effect of polymer plate on blast wave decreases gradually.

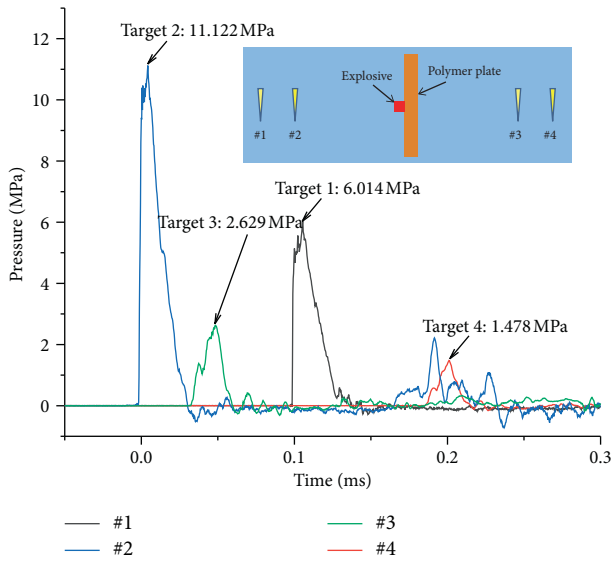

Figure 12: Shock wave pressure curve of the polymer plate C3 under 8 g explosive.

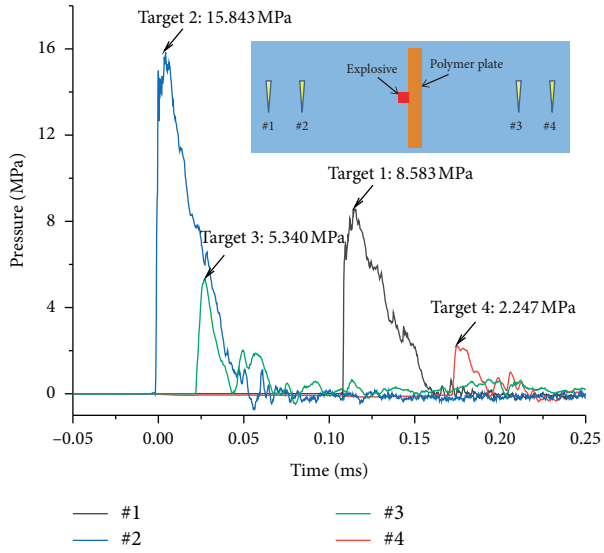

Figure 13: Shock wave pressure curve of the polymer plate C5 under 20 g explosive.

4. Underwater Near-Field Explosion Tests

In order to study the influence of explosive quantity on the damage characteristics of polymer plates under the impact of the underwater near-field explosion, the underwater near-field explosion tests of polymer plates N1–N4 were carried out under four different explosive quantities. In the test, the center of the polymer plate, the rock emulsion explosive, and the underwater shock wave sensors are in the same horizontal line, and the explosive is fixed at 200 mm away from the plate center, as shown in Figure 17.

4.1. Failure Characteristics. As shown in Figure 18, under the action of an underwater near-field explosion of a single detonator, the damage mode of polymer plate N1 is local damage. Under the impact of the near-field explosion, there is a small area of penetration failure in the upper right of the plate, and a circular spalling failure area with a diameter of 107 mm appears. When the compression wave in the plate is transmitted to the bottom of the plate, the reflection forms a tensile wave, which makes the plate spall. Because the left and right sides of the polymer plate are fixed, when the plate is subjected to a shock wave, a crack parallel to the fixed boundary is generated, which extends from the upper top surface to the lower bottom surface of the plate. Under the impact of 0 g explosive, the polymer plate N1 is still an independent whole, and the residual area is 99.86% of the original area.

When the explosive amount increased to 5 g, the polymer plate N2 was completely broken. As shown in Figure 19, there is a penetrating failure in the center of polymer plate N2, and a circular collapse failure area with a diameter of about 173 mm is produced. After the initiation of explosive, the polymer plate is impacted, and the plate is subjected to radial tensile action, while the tensile strength of the polymer plate is less than the tensile stress produced by the explosion, so there are many radial cracks on the surface of the plate, which extend to the edge of the specimen and split the plate into different sizes of fragments. At the same time, there are also longitudinal cracks at the fixed boundary on both sides of the plate, which is because the polymer plate will form a large tensile stress at the fixed boundary when it is impacted by an explosion. The largest residual area of the plate accounts for 21.55% of the total area of the original polymer plate, the smallest area accounted for 1.08%, and the total residual area accounts for 99.52%.

When the amount of explosive is 10 g, the specimen N3 is completely broken and loses strength, as shown in Figure 20. After the explosion of the rock emulsion explosive, the huge pressure is released in a very short time, and a sudden pressure jump occurs around the explosion point. The distance between the explosive source and the polymer plate is only 200 mm. After the explosive explosion, the compressive pulse load with a high peak value and short duration will be generated on the specimen, which will reflect and produce tensile waves on the specimen surface, resulting in the fracture of the specimen structure. The largest area, the smallest area, and the total residual area account for 13.72%, 1.13%, and 73.34% of the original area, respectively.

As shown in Figure 21, when the rock emulsion explosive is 20 g, the polymer plate N4 is completely destroyed, and the fragments in the middle of the plate are too small to pick up, only the two boundaries in the channel are relatively complete. The largest block area, the smallest block area, and the total residual area accounted for 15.20%, 5.63%, and 48.44% of the original area, respectively.

Figures 18–21 show the damage results of polymer plates by different mass rock emulsion explosives under the action of underwater near-field explosions. With the increase of explosive quantity, the damage mode of polymer plates changes from local damage to complete damage. Under the impact of the underwater near-field explosion, penetration failure occurs in the central region

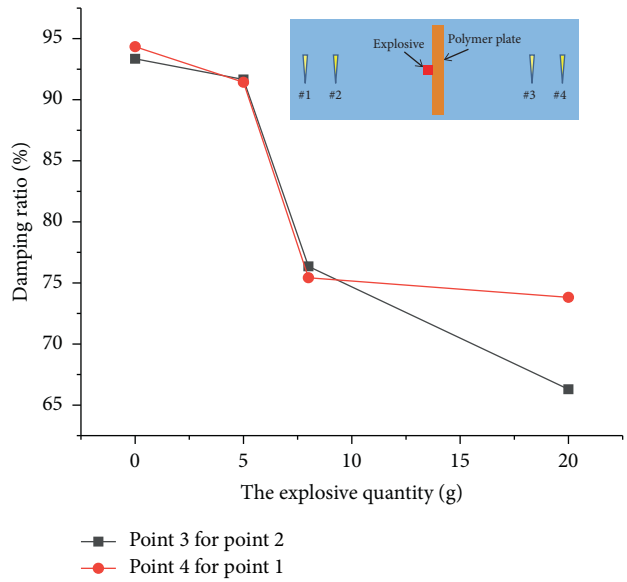

Figure 14: Attenuation ratio of measuring points at the same distance from the detonation source.

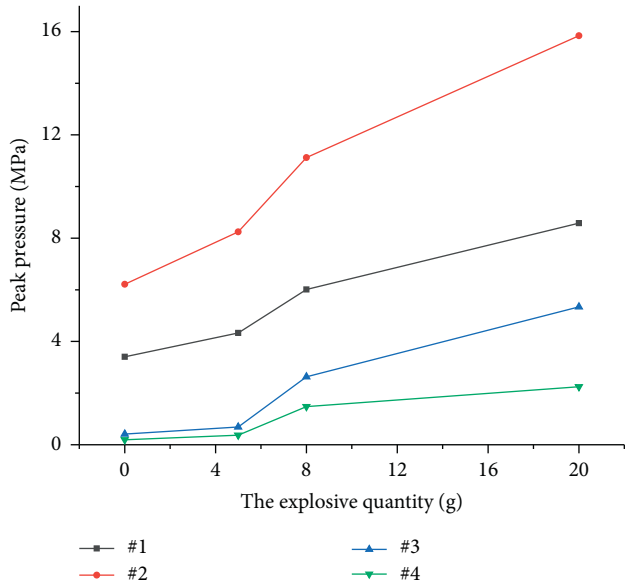

Figure 15: Peak pressure curve of shock wave under contact explosion.

of the plate, and the area of penetration failure increases with the increase of explosive quantity. The residual area of specimens with different explosive amounts is statistically analyzed. As shown in Table 3, the residual area of plates with explosive amounts of 5 g, 10 g, and 20 g decreases by 0.34%, 26.55%, and 51.50%, respectively, compared with that with explosive amounts of 0 g. The maximum residual area decreases by 78.42%, 86.26%, and 84.78%, respectively, relative to the explosive amount of 0 g. With the increase of explosive quantity, the energy produced by the explosion increases gradually, and the residual area and maximum fragment area decrease gradually.

4.2. Shock Wave Propagation Characteristics. In order to analyze the change of peak pressure before and after the polymer plate under different explosive quantities, four measuring points 1–4 are arranged before and after the polymer plate to measure the pressure time history curve at the measuring points, as shown in Figure 22. The measuring points 1 and 2 and rock emulsion explosive are on the same side of the polymer plate, while the measuring points 3 and 4 are on the other side of the polymer plate.

When the explosion load is only a single detonator, the pressure time history curves at four measuring points are shown in Figure 22. The peak pressure at measuring point 2 is the largest, and it decays rapidly after reaching the peak value, and several peaks appear, and the peak value gradually decreases and finally tends to be flat. The main reason is that the underwater explosion shock wave transmits and scatters on the plate surface for many times, which leads to the fluctuation and multipeak phenomenon of the pressure time history curve. It can be seen from Figure 22 that under the action of underwater contact explosion load, the peak pressures at the four measuring points 1–4 are 4.032 MPa, 7.518 MPa, 0.944 MPa, and 0.215 MPa, respectively, and the peak pressures at the measuring points behind the plate are far less than those at the measuring points in front of the plate. Compared with point 2, the peak pressure of point 3 decreases by 87.44%. And the measuring point 4 is reduced by 94.67% compared with point 1. It should be noted that when the explosive explodes, the instrument has been triggered and started to record. 0 s in the figure is not the initiation time of emulsion explosive, but the time interval between different measuring points reaching the peak pressure is not affected by the start recording time. The time interval between the peak pressures of measuring points 2 and 3 is 0.236 ms, and the time interval between the peak pressures of measuring points 1 and 4 is 0.219 ms.

Figure 23 shows the shock wave pressure curves at four measuring points when the explosive quantity is 5 g, and the waveform is similar to that when the explosive quantity is 0 g. The peak pressures of 1–4 are 6.143 MPa, 13.525 MPa, 1.909 MPa, and 1.442 MPa, respectively. The peak pressure of point 3 is 85.59% lower than that of point 2, and that of point 4 is 76.53% lower than that of point 1. The time interval between the peak pressure of measuring points 2 and 3 is 0.248 ms, and the time interval between the peak pressure of measuring points 1 and 4 is 0.234 ms. The time of peak pressure at measuring points 3 and 4 is later than that at measuring points 2 and 1, respectively, which means that the existence of polymer plate delays the time of peak pressure at measuring points 3 and 4.

When the explosive quantity is 10 g, the pressure time history curve at the measuring point is shown in Figure 24. It can be seen from the figure that the pressure peak values of the measuring points from large to small are 18.278 MPa, 8.223 MPa, 2.496 MPa, and 1.598 MPa, respectively, corresponding to measuring point 2, measuring point 1, measuring point 3, and measuring point 4. The peak pressure of point 3 decreases by 86.34% compared with point 2, and the peak pressure of point 4 decreases by 80.57% compared with point 1. The time interval between the peak pressure of

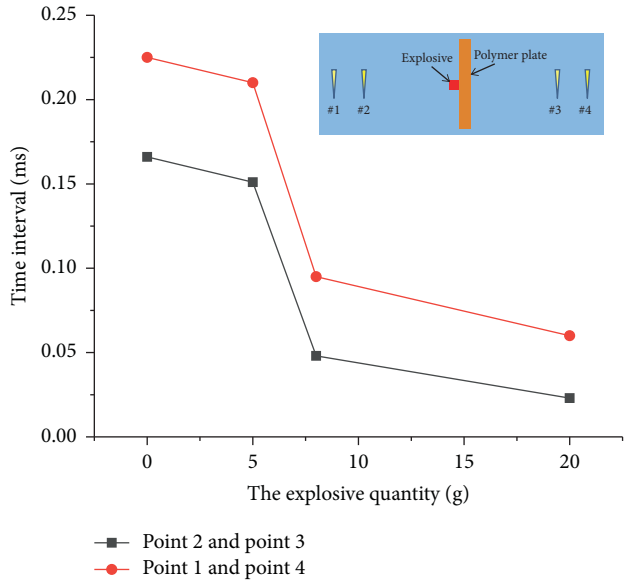

Figure 16: Time interval of pressure peak at different measuring points.

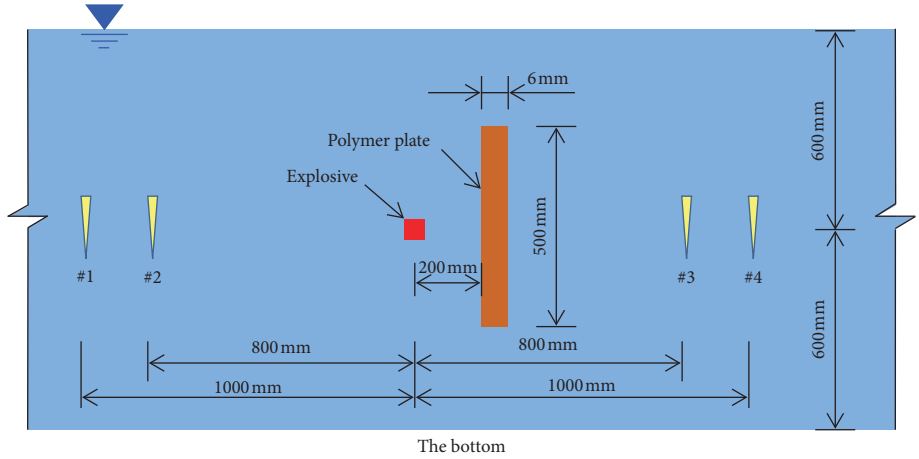

Figure 17: Schematic diagram of near-field explosion.

measuring points 1 and 4 is 0.264 ms, and the time interval between the peak pressure of measuring points 2 and 3 is 0.245 ms.

In order to better analyze the peak pressure variation law of each measuring point under different amounts of primary explosive, the peak pressure variation curves of measuring points 1–4 under different amounts of primary explosive are shown in Figure 25. It can be seen from Figure 25 that the peak value of each measuring point increases with the increase of explosive quantity. The peak value and growth rate of measuring points 1 and 2 are significantly higher than those of measuring points 3 and 4. When the explosive quantity changes, the attenuation ratio of measuring point 3 relative to measuring point 2 and measuring point 4 relative to measuring point 1 shows a decreasing trend on the whole, but the decreasing rate of attenuation ratio is small; i.e., the reducing effect of polymer plate on shock wave is less affected by the explosive quantity.

It can be seen from Figures 22–24 that under the action of the underwater near-field explosion, the peak pressure and the time required to reach the peak pressure at measuring points 3 and 4 are less than those at measuring points 2 and 1. As shown in Table 4, under different amounts of explosive, the time interval for measuring points with the same distance from the explosive to reach the peak pressure is counted. With the increase of explosive quantity, the time interval changed little. Under the action of underwater near-field explosion load, the delay effect of polymer plate on explosion shock wave is less affected by the amount of explosive.

5. Comparative Analysis of Underwater Near-Field and Contact Explosion

Three control groups (C1 and N1; C2 and N2; C4 and N4) were used to compare and analyze the damage

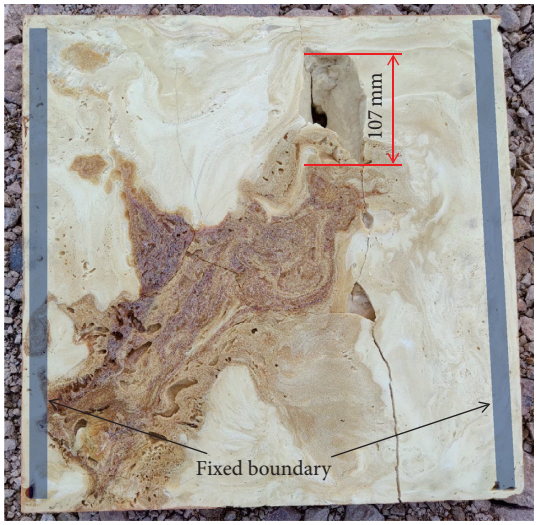

Figure 18: Test results of the polymer plate N1 under 0 g explosive (only one nonconductive detonator).

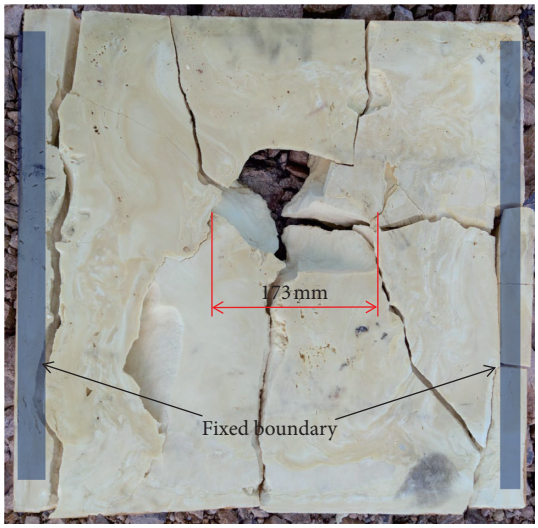

Figure 19: Test results of the polymer plate N2 under 5 g explosive.

Figure 20: Test results of the polymer plate N3 under 10 g explosive.

Figure 21: Test results of the polymer plate N4 under 20 g explosive.

characteristics of polymer plates under underwater contact and near-field explosion loads with different explosives. In the process of underwater near-field explosion test for plate N4 when the explosive quantity is 20 g, the shock wave data were not measured at the four measuring points due to instrument reasons.

5.1. Failure Modes. It can be seen from Figures 7 and 8 that under the action of underwater contact explosion load, the explosive quantity increases from 0 g to 5 g, and the polymer plate directly changes from the middle through failure to complete failure. When a 20 g explosive is used to conduct a contact explosion test on plate C4, the plate is completely crushed. When the amount of explosive is 0 g–20 g, the polymer plates are subjected to an underwater contact explosion test, and the plates are damaged as a whole.

It can be seen from Figures 18, 19, and 21 that, under the action of an underwater near-field explosion, the polymer plate is changed from local through failure to overall failure. Under the action of a single nonconductive detonator explosion load, local penetration failure of plate N1 occurs, and the plate is still intact. However, when the explosive amount is increased to 5 g, the plate N2 is completely broken and loses its stiffness and strength.

In the underwater explosion test of polymer plate with different weights of rock emulsion explosive, the change rule of residual area ratio (i.e., the percentage of residual area in the original area) is shown in Figure 26. The residual area ratio of polymer plate in the near-field explosion is larger than that in contact explosion. Under the conditions of two kinds of blasting center distances, with the increase of the amount of rock emulsion explosive, the damage of the plate caused by the blast wave increases gradually, and the residual area ratio of the plate decreases gradually. Compared with the underwater near-field explosion, the underwater contact

Table 3: Residual area of polymer plate under near-field explosion.

The explosive quantity	0 g	5 g	10 g	20 g
Residual area (mm^2)	249650	248801	183359	121091
Maximum fragmentation area (mm^2)	249650	53871	34312	38004
Minimum fragmentation area (mm^2)	0	2699	2818	14083
Residual area ratio (%)	99.86	99.52	73.34	48.44

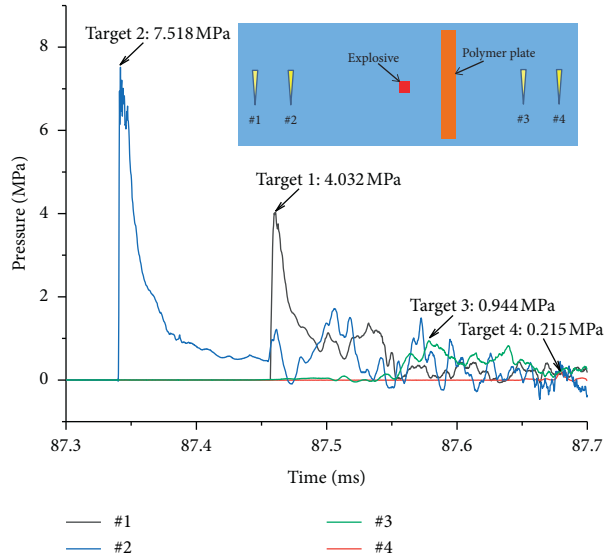

Figure 22: Shock wave pressure curve of the polymer plate N1 under 0 g explosive.

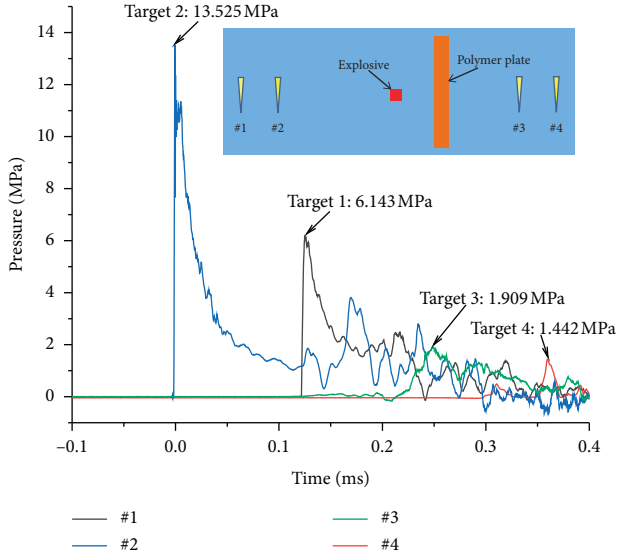

Figure 23: Shock wave pressure curve of the polymer plate N2 under 5 g explosive.

explosion with the same amount of explosives causes more damage to the polymer plate. This is because the compressibility of the water medium is small, and the shock wave generated by the underwater explosion has the characteristics of high peak pressure and short duration. When the explosive explodes on the surface of the plate, in addition to the explosion product directly acting on the plate, it is also affected by the shock wave in the water. In a near-field explosion, the peak pressure of the shock wave near the explosive is relatively large. As the propagation distance increases, the peak pressure of the shock wave gradually decreases.

5.2. Shock Wave Propagation Characteristics. It can be seen from Figure 27 that, under the action of underwater contact explosion, the peak pressure at the measuring point is less than that of near-field explosion under the same explosive quantity, and the peak pressure at the measuring point increases gradually with the increase of explosive quantity. When the explosive quantity increases from 0 g to 5 g, the peak pressure of point 2 under underwater contact explosion load increases from 6.213 MPa to 8.245 MPa, an increase of 32.7%; while the peak pressure of point 2 increases from 7.518 MPa to 13.525 MPa under the underwater near-field contact explosion load, an increase of 79.9%. Under the same conditions, with the increase of explosive quantity, the peak pressure of underwater near-field explosion increases more greatly. Under the condition of underwater near-field, the polymer plate has less influence on the propagation of explosion shock waves.

In underwater contact and near-field explosion, the damage of polymer plate consumes most of the energy generated by the explosion. Only a small amount of shock wave can penetrate the plate and continue to propagate in the form of the shock wave in the medium behind the plate. Table 5 shows the attenuation ratio of the shock wave pressure peak of point 3 to point 2 and point 4 to

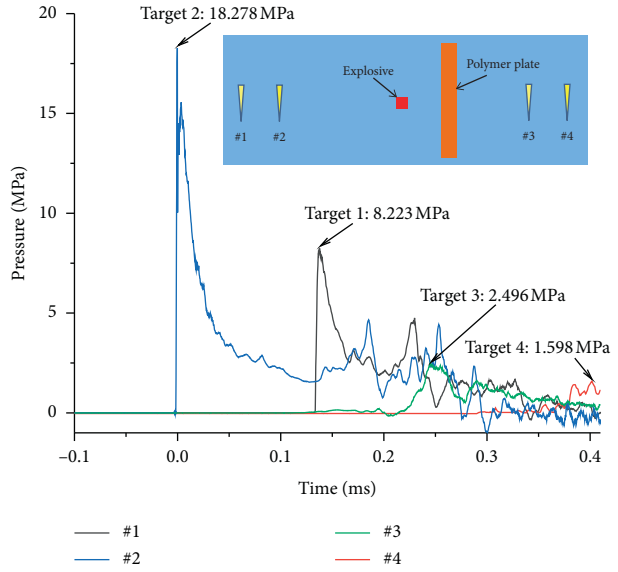

Figure 24: Shock wave pressure curve of the polymer plate N3 under 10 g explosive.

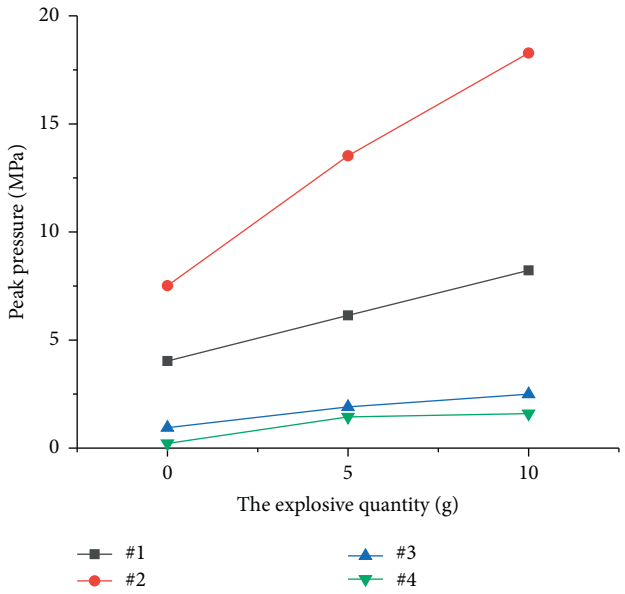

Figure 25: Peak pressure curve of shock wave under near-field explosion.

Table 4: Time interval of peak pressure at different measuring points.

The explosive quantity (g)	Time interval (ms)	
	Point 2 and point 3	Point 1 and point 4
0	0.236	0.219
5	0.248	0.234
10	0.245	0.264

point 1 under underwater contact and near-field explosion when the explosive quantity is 0 g and 5 g. It can be seen from Table 5 that under the action of underwater contact explosion, the relative attenuation ratio of different measuring points is greater than that of near-field explosion. Therefore, under the action of underwater

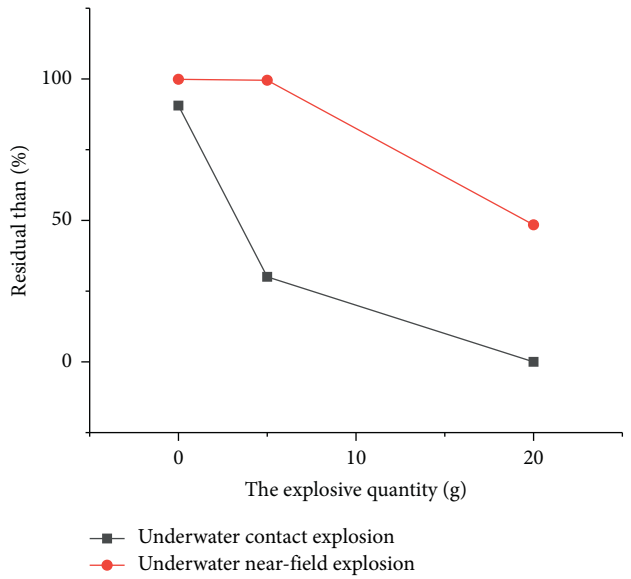

Figure 26: Residual area ratios under different explosive quantities.

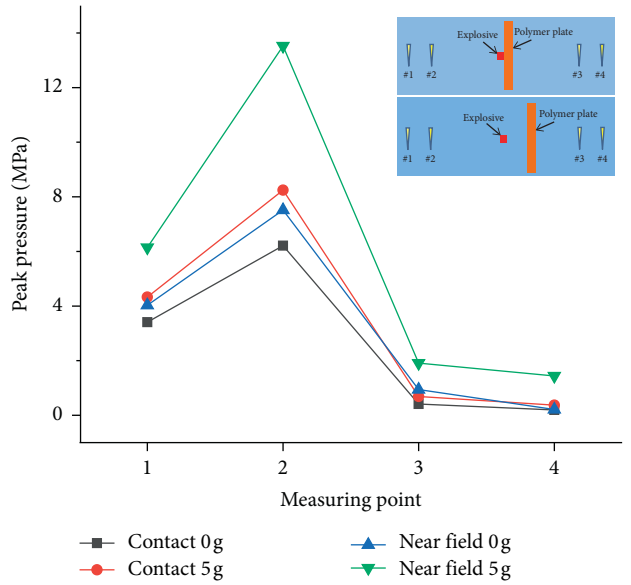

Figure 27: Pressure peaks at measuring points in underwater contact and near-field explosion under different explosive quantities.

Table 5: Attenuation ratio of peak pressure at measuring points.

Working condition	The explosive quantity (g)	Point 3 for point 2	Point 4 for point 1
Underwater contact tests	0	93.35%	94.34%
	5	91.66%	91.43%
Underwater near-field tests	0	87.44%	94.67%
	5	85.59%	76.53%

contact explosion, the destruction of polymer plate consumes more energy and the plate has a stronger effect on reducing shock wave.

6. Conclusions

Through the method of field explosion test, the underwater near-field and contact explosion tests were carried out on eight polymer plates. The failure modes and propagation characteristics of explosion shock waves of polymer plates under the action of underwater contact and near-field explosion were compared and analyzed. The conclusions are summarized in the following:

(1) The polymer plates subjected to contact underwater explosion are mainly overall failure and lose their strength and stiffness. With the increase of explosive quantity, the residual area ratio of the specimen decreases gradually. The polymer plate has the effect of reducing and delaying the blast wave, which is significant when the explosive quantity is small, but with the increase of the explosive quantity, the reducing and delaying effect decreases rapidly

(2) Under the loading of the underwater near-field explosion, with the increase of explosive quantity, the damage mode of the polymer plate changes from local through damage to overall damage. The polymer plate also has the effect of reducing and delaying the shock wave of the underwater near-field explosion, but the influence strength is less affected by the amount of explosive

(3) Compared with the underwater near-field explosion, an underwater contact explosion with the same amount of explosive will cause greater damage to the polymer plate and smaller residual area. Under the action of an underwater contact explosion, the peak pressure at the measuring point is less than that of a near-field explosion under the same amount of explosive

Data Availability

All the data are included within the article in tables and figures.

Conflicts of Interest

The authors declare that they have no conflicts of interest.

Acknowledgments

The authors gratefully appreciate the support from the National Natural Science Foundation of China (52009126), Key Scientific Research Projects of Colleges and Universities in Henan Province (21A570006), the Outstanding Young Talent Research Fund of Zhengzhou University (1621323001), and China Postdoctoral Science Foundation (2020M672311 and 2020T130569).

References

[1] R. Wang, F. Wang, J. Xu, Y. Zhong, and S. Li, "Full-scale experimental study of the dynamic performance of buried drainage pipes under polymer grouting trenchless rehabilitation," *Ocean Engineering*, vol. 181, pp. 121–133, 2019.

[2] H. Fang, B. Li, F. Wang, Y. Wang, and C. Cui, "The mechanical behaviour of drainage pipeline under traffic load before and after polymer grouting trenchless repairing," *Tunnelling and Underground Space Technology*, vol. 74, pp. 185–194, 2018.

[3] F. Wang, C. Guo, and Y. Gao, "Formation of a polymer thin wall using the level set method," *International Journal of Geomechanics*, vol. 14, no. 5, Article ID 4014021, 2014.

[4] J. Y. Chen, O. Ummin, T. Yu, and Y. J. Qi, "Applications of Rayleigh wave detection technique and polymer grouting technology in waterproof construction," *Applied Mechanics and Materials*, vol. 405–408, pp. 748–754, 2013.

[5] S. R. Iyengar, E. Masad, A. K. Rodriguez, H. S. Bazzi, D. Little, and H. J. M. Hanley, "Pavement subgrade stabilization using polymers: characterization and performance," *Journal of Materials in Civil Engineering*, vol. 25, no. 4, pp. 472–483, 2013.

[6] S. Saleh, N. Z. M. Yunus, K. Ahmad, and N. Ali, "Improving the strength of weak soil using polyurethane grouts: a review," *Construction and Building Materials*, vol. 202, pp. 738–752, 2019.

[7] F. M. Wang, M. S. Shi, H. J. Li, and Y. H. Zhong, "Experimental study on the anti-permeability properties of polymer grouting materials," *Advanced Materials Research*, vol. 284–286, pp. 1952–1955, 2011.

[8] J. Chen, X. Yin, H. Wang, and Y. Ding, "Evaluation of durability and functional performance of porous polyurethane mixture in porous pavement," *Journal of Cleaner Production*, vol. 188, pp. 12–19, 2018.

[9] G. Harikrishnan and D. V. Khakhar, "Effect of monomer temperature on foaming and properties of flexible polyurethane foams," *Journal of Applied Polymer Science*, vol. 105, no. 6, pp. 3439–3443, 2007.

[10] M. Shi, F. Wang, and J. Luo, "Compressive strength of polymer grouting material at different temperatures," *Journal of Wuhan University of Technology-Materials Science Edition*, vol. 25, no. 6, pp. 962–965, 2010.

[11] M. Li, M. Du, F. Wang, B. Xue, C. Zhang, and H. Fang, "Study on the mechanical properties of polyurethane (PU) grouting material of different geometric sizes under uniaxial compression," *Construction and Building Materials*, vol. 259, Article ID 119797, 2020.

[12] C. Guo, B. Sun, D. Hu, F. Wang, M. Shi, and X. Li, "A field experimental study on the diffusion behavior of expanding polymer grouting material in soil," *Soil Mechanics and Foundation Engineering*, vol. 56, no. 3, pp. 171–177, 2019.

[13] C. Wang, Q. Liu, C. Guo et al., "An experimental study on the reinforcement of silt with permeable polyurethane by penetration grouting," *Advances in Civil Engineering*, vol. 2020, Article ID 8834331, 14 pages, 2020.

[14] R. Valentino, E. Romeo, and D. Stevanoni, "An experimental study on the mechanical behaviour of two polyurethane resins used for geotechnical applications," *Mechanics of Materials*, vol. 71, pp. 101–113, 2014.

[15] M. C. Saha, H. Mahfuz, U. K. Chakravarty, M. Uddin, E. Kabir, and S. Jeelani, "Effect of density, microstructure, and strain rate on compression behavior of polymeric foams,"

Materials Science and Engineering A, vol. 406, no. 1-2, pp. 328–336, 2005.

[16] V. Kumar, K. V. Kartik, and M. A. Iqbal, "Experimental and numerical investigation of reinforced concrete slabs under blast loading," *Engineering Structures*, vol. 206, Article ID 110125, 2020.

[17] W. Wang, D. Zhang, F. Lu, S.-C. Wang, and F. Tang, "Experimental study on scaling the explosion resistance of a one-way square reinforced concrete slab under a close-in blast loading," *International Journal of Impact Engineering*, vol. 49, pp. 158–164, 2012.

[18] W. Wang, D. Zhang, F. C. Lu, and F. Tang, "Experimental study and numerical simulation of the damage mode of a square reinforced concrete slab under close-in explosion," *Engineering Failure Analysis*, vol. 27, pp. 41–51, 2013.

[19] C. Wu, L. Huang, and D. J. Oehlers, "Blast testing of aluminum foam-protected reinforced concrete slabs," *Journal of Performance of Constructed Facilities*, vol. 25, no. 5, pp. 464–474, 2011.

[20] J. Li, C. Wu, H. Hao, Z. Wang, and Y. Su, "Experimental investigation of ultra-high performance concrete slabs under contact explosions," *International Journal of Impact Engineering*, vol. 93, pp. 62–75, 2016.

[21] X. Yu, B. Zhou, F. Hu et al., "Experimental investigation of basalt fiber-reinforced polymer (BFRP) bar reinforced concrete slabs under contact explosions," *International Journal of Impact Engineering*, vol. 144, Article ID 103632, 2020.

[22] K. Ohkubo, M. Beppu, T. Ohno, and K. Satoh, "Experimental study on the effectiveness of fiber sheet reinforcement on the explosive-resistant performance of concrete plates," *International Journal of Impact Engineering*, vol. 35, no. 12, pp. 1702–1708, 2008.

[23] X. Zhao, G. Wang, W. Lu, G. Yang, M. Chen, and P. Yan, "Experimental investigation of RC slabs under air and underwater contact explosions," *European journal of environmental and civil engineering*, vol. 25, no. 1, pp. 190–204, 2021.

[24] Q. Yan, C. Liu, J. Wu, J. Wu, and T. Zhuang, "Experimental and numerical investigation of reinforced concrete pile subjected to near-field non-contact underwater explosion," *International Journal of Structural Stability and Dynamics*, vol. 20, no. 6, Article ID 2040003, 2020.

[25] G. Yang, G. Wang, W. Lu, X. Zhao, P. Yan, and M. Chen, "Cross-section shape effects on anti-knock performance of RC columns subjected to air and underwater explosions," *Ocean Engineering*, vol. 181, pp. 252–266, 2019.